J Therm Anal Calorim (2012) 108:101–108
DOI 10.1007/s10973-011-1613-7

Crystallinity of Dynasan®114 and Dynasan®118 matrices for the production of stable Miglyol®-loaded nanoparticles

Patrícia Severino · Samantha C. Pinho · Eliana B. Souto · Maria H. A. Santana

Received: 27 March 2011 / Accepted: 19 April 2011 / Published online: 4 May 2011

Abstract This study focuses on the physicochemical characterization of lipid materials useful for the production of the so-called solid lipid nanoparticles (SLN) and nanostructured lipid carriers (NLC). The chosen lipids were Dynasan®114 (glyceril trimyristate) and Dynasan®118 (glyceril tristearate) as solid lipids (SL), melting temperature above 80 °C, and Miglyol®812 (caprylic/capric triglyceride) and Miglyol®840 (propylene glycol dicaprylate/dicaprate) as liquid lipids (LL), crystallizing below −15 °C. Raw lipids (pure or SL:LL mixtures) were analyzed by differential scanning calorimetry (DSC), wide angle X-ray diffraction (WAXD), and Polarized Light Microscopy (PLM), before and after tempering at 80 °C for 1 h. The selected SL:LL combination was 70% (Dynasan®114 and 118) and 30% (Miglyol®812 and 840) for the production of SLN and NLC by high-pressure homogenization (HPH), respectively. Particles with a mean size of 200 nm (polydispersity index <0.329) and zeta potential of −15 mV were obtained, and their long-term stability was confirmed for 3 months of storage at 7 °C.

Keywords Dynasan®114 · Dynasan®118 · Miglyol®812 · Miglyol®840 · Differential scanning calorimetry · Wide angle X-ray diffraction · Polarized light microscopy · Lipid nanoparticles

P. Severino · M. H. A. Santana (✉)
Department of Biotechnological Processes, School of Chemical Engineering, State University of Campinas (UNICAMP), Av. Albert Einstein, 500 São Paulo, Campinas 13083-970, Brazil
e-mail: lena@feq.unicamp.br

P. Severino · E. B. Souto (✉)
Faculty of Health Sciences, Fernando Pessoa University (FCS-UFP), Rua Carlos da Maia, 296, 4200-150 Porto, Portugal
e-mail: eliana@ufp.edu.pt

S. C. Pinho
Faculty of Animal Science and Food Engineering, University of São Paulo (USP), São Paulo, Brazil

E. B. Souto
Institute of Biotechnology and Bioengineering, Centre of Genomics and Biotechnology, University of Trás-os-Montes and Alto Douro (CGB-UTAD/IBB), P.O. Box 1013, 5001-801 Vila Real, Portugal

Introduction

Nanoparticles have become a rapidly growing field with potential applications in health and drug therapy [1]. Examples include solid lipid nanoparticles (SLN) [2], nanostructured lipid carrier (NLC) [3], liposomes [4], polymeric nanoparticles [5], and dendrimers [6], provided by their extraordinary physical and chemical properties resulting from the nanosize effect [7]. Lipid nanoparticles (SLN and NLC) are considered the least toxic among all the other nanoparticles for in vivo applications. SLN and NLC have been proposed as alternative drug carriers because of their physiological lipid composition, the variety of possible administration routes (e.g., intravenous, oral, and topical), large scale production by HPH, and the relatively low cost of the excipients. A number of studies have recently been published, focusing on the production of SLN and NLC, and their physicochemical characterization, release profile, including the feasibility of incorporation of lipophilic and hydrophilic drugs [7, 8].

Lipids employed for the production of nanoparticles include triglycerides and their mixtures, fatty acids, and

waxes [9]. It is, however, required that matrix maintains the solid state at room temperature, and for this purpose, the selection of lipids requires the evaluation of their polymorphic, crystallinity, miscibility, and physicochemical structure. For large production, the control of polymorphism is demanded because of its influence on the encapsulation efficiency and on the drug expulsion during storage [10–12]. The lipid crystallization is also an important characteristic, since the crystalline structures of triglycerides (e.g., Dynasan®114 and Dynasan®118) can occur in different polymorphic forms (α, β', and β). The α-form (hexagonal) is the least stable with a lower melting point and latent heat, whereas the β-form (triclinic) is more stable with higher melting point and higher latent heat. The transformation of α to β' (orthorhombic) and β is irreversible, and occurs toward a more hydrodynamic stable system [12].

In the pharmaceutical field, lipid nanoparticles can be used for all administration routes because of their small particle size, ranging from 50 to 1000 nm [9, 13–15]. Up to now, a variety of techniques have been employed for lipid nanoparticle production [16]. The most promising technique to achieve higher drug loading in nanoparticles is the high-pressure homogenization (HPH). This process is easy to scale up, it does not use organic solvents, and produces particles with small diameter [17, 18] and low polydispersity index [19]. High-shear homogenization followed by the HPH can modulate the mean nanoparticle size. Furthermore, different lipid combinations can be tested to obtain the preferred release profile [20, 21]. HPH has been used for more than 50 years for the production of emulsions for parenteral nutrition, such as Intralipid® and Lipofundin®.

The aim of this study was to evaluate the polymorphism and crystallinity of triglycerides commonly used in the production of SLN and NLC, such as trimiristin (Dynasan®114) and tristearin (Dynasan®118), and the binary mixture of solid and liquid lipids, such as caprylic/capric triglyceride (Miglyol®812) and propylene glycol dicaprylate/dicaprate (Miglyol®840).

Materials and methods

Material

Trimyristin (Dynasan®114), Tristearin (Dynasan®118), Caprylic/Capric Triglycerides (Miglyol®812), and Propylene Glycol Dicaprylate/Dicaprate (Miglyol®840) were obtained from Sasol Olefins & Surfactants (Germany). Polysorbate 80 (Tween®80) was obtained from Synth (Brazil). Double-distilled water was used after filtration in Millipore systems (home-supplied).

Methods

Lipid screening and thermal treatment of lipid materials

The solid lipid (Dynasan®114 and Dynasan®118) and the binary mixture of solid and liquid lipids (Miglyol®812 and Miglyol®840) were combined in different ratios and analyzed separately. Samples were analyzed before and after tempering at 80 °C for 1 h. Tempering at 80 °C was preselected since lipid nanoparticles are generally produced at a temperature 10 °C above the melting point of solid lipids. This process consisted of melting at 80 °C on a thermostatic bath (Marconi, MA 127/BD, Brazil), following tempering by sample incubation in the same thermostatic bath for 1 h at 80 °C [22]. The samples were then kept at room temperature until complete cooling and solidification, to check for the creation of polymorphic forms. Most production processes of SLN and NLC require heating; thus, tempering was performed to mimic the production procedure carried out for lipid nanoparticles production.

Preparation of lipid nanoparticles

SLN and NLC were prepared by HPH (NiroSoavi, Panda, Italy) [23]. The experimental protocol was to melt the lipid or its mixtures 10 °C above the melting point of solid lipid, and simultaneously, an aqueous solution containing the surfactant was heated at the same temperature. The molten lipid phase was dispersed in aqueous surfactant solution applying high-shear homogenization (Ultra-Turrax® T25, USA) at 15.000 rpm for 3 min to obtain a microemulsion. Then, the microemulsion was passed three times at 500 bar through the hot HPH. After that, the formulation was cooled in an ice bath to allow lipid recrystallization until reaching the temperature of 20 °C. Table 1 shows the developed formulation.

Differential scanning calorimetry (DSC)

Thermal behavior of lipid matrices was analyzed by DSC (Mettler Toledo, FP90 Central Processor, São Paulo, Brazil). A volume of the sample containing approximately 5–10 mg of lipid mass was weighed in an aluminum pan and sealed hermetically, under inert atmosphere (N_2). The analysis was performed at the heating and cooling rates of 5 K/min, using an empty pan as reference. The samples were heated up from 10 °C to 100 °C, after being cooled down to 10 °C Table 2.

Wide angle X-ray diffraction (WAXD)

To study the polymorphism and crystalline properties of the lipids and their mixtures, WAXD was carried out in a

Table 1 Composition of lipid mixtures in percentage (w/w)

Sample	Dynasan®114	Dynasan®118	Miglyol®812	Miglyol®840
D4M812/90:10	90		10	
D4M812/80:20	80		20	
D4M812/70:30	70		30	
D4M840/90:10	90			10
D4M840/80:20	80			20
D4M840/70:30	70			30
D8M812/90:10		90	10	
D8M812/80:20		80	20	
D8M812/70:30		70	30	
D8M840/90:10		90		10
D8M840/80:20		80		20
D8M840/70:30		70		30

Table 2 Composition of solid lipid nanoparticles (SLN) values in percentage (w/w)

Phase	Formulation	1[a]	2[a]	3[a]	4[a]
Oil	Dynasan®114	2.1		2.1	
	Dynasan®118		2.1		
	Miglyol®812	0.9	0.9		
	Miglyol®840			0.9	0.9
Aqueous	Tween®80	3	3	3	3
	Water	200	200	200	200

[a] Values in percentage

diffractometer X-ray (Philips, model X'pert, Pennsylvania, USA), using copper anode which delivered an X-ray of wavelength, $\lambda = 0.154056$ nm. WAXD measurements were taken from 50° to 330° in 0.015° steps (1 s per step). The interlayer spacings were calculated from the reflections using Bragg's equation:

$$d = \frac{\lambda}{\text{sen } 2\theta}$$

where λ is the wavelength of the incident X-ray beam, and θ is the scattering angle. The parameter d, otherwise called the interlayer spacing, is the separation between a particular set of planes of the crystal–lattice structure. Data of the scattered radiation were recorded using a blend local-sensible detector with an anode voltage of 40 kV, a current of 25 mA, and a scan rate of 0.5°/min. The samples were mounted on a thin glass capillary being fastened to a brass pin without any previous sample treatment.

Polarized light microscopy (PLM)

Polarized light microscopy (PLM) is used for checking for lipid microstructures and monitoring their molten transitions and fusion. Micrographs of crystallizing lipid mixtures were examined with a photomicroscope (LEICA, model Leitz DMRXE, Bensheim, Germany) coupled with a software Motic Images Advanced 3.2 and cross polarizer. Samples were evaluated 24 h after production and analyzed with increase of 20,000×.

Particle size and zeta potential analysis

The mean particle size was determined through dynamic light scattering (DLS, Zetasizer Nano NS, Malvern Instruments, Malvern, UK). DLS, sometimes referred to as photon correlation spectroscopy (PCS), is a non-invasive, well-established technique for measuring the size of molecules and particles typically in the submicron region [24]. This instrument also allows determining the zeta potential by electrophoretic mobility of particles in an electrical field. The samples were diluted with ultra-purified water to weaken the opalescence before measuring the particle mean diameter and polydispersity index. Zeta potential of lipid nanoparticles was also measured in purified water adjusting conductivity (50 μS/cm) with potassium chloride solution (0.1%, w/v). The zeta potential was determined from the electrophoretic mobility using the Helmholtz–Smoluchowski equation [25]. The processing was done by the software included within the system.

Results

Polymorphic behavior is often shown by long-chain compounds, in general, those compounds crystallize in two or three different phases, α and β', or α, β', and β, respectively. DSC was employed to study the melting temperature and crystallization behavior of lipids [26]. For this study, 12 samples were analyzed using different ratios of Dynasan®114 and Dynasan®118 as solid lipids and

Miglyol®812 and Miglyol®840 as liquid lipids, according to Table 1.

According to the results obtained after DSC analysis (Table 3), Dynasan®114 and Dynasan®118 depicted melting events at 60.7 °C and 73.8 °C, respectively, and the onset temperatures at 57.0 °C and 60.9 °C, respectively. The difference between the melting and the onset temperatures is the range at which the melting event of the lipid occurs, and the greater the difference, the greater the disorder of the crystals. After adding the liquid lipid (Miglyol®812 or Miglyol®840) to the solid lipid (Dynasan®114 or Dynasan®118), this difference increased, as observed for the samples D4M812 (70:30); D4M812 (70:30); D8M812 (70:30); and D8M840 (70:30). It should be pointed out that Miglyol®812 and Miglyol®840 mainly differ in C_8/C_{10}-ratio. Because of its low C_{10}-content, the viscosity and cloud point of Miglyol 812 is lower. As shown in Table 3, the melting range of all the formulations was recorded between 54 and 72 °C.

Using 30% of liquid lipid, major differences between the temperatures were recorded, favoring a less orderly, lipid matrix containing imperfections in their structure, capable of accommodating a larger amount of drug, to minimize its expulsion during storage, and also to modulate their release pattern [9, 20]. In colloidal systems, for in vivo use, it is desired to work with lipids having onset temperatures above 40 °C, to avoid melting of the nanoparticles when administered [27].

The samples chosen to undergo tempering are presented in Table 4 which also shows the melting temperatures and onset temperature, before and after the tempering process, and the differences between them. The melting and the onset temperatures fusion of each lipid mixture subjected to tempering was obtained from the DSC thermograms. When comparing the differences between the melting and onset temperatures, before and after tempering, an increase occurred after tempering. These results show that these structures exhibit susceptibility to clutter after processing for production of lipid nanoparticles. This disruption facilitates the encapsulation of drugs and increases particle stability during storage. After tempering, the obtained melting temperatures were higher than 40 °C, which represents an important property, because it ensures the integrity of the particles for parenteral use [28, 29].

In general, the lipids crystallize in two or three different phases, α and β' or α, β, and β'. To analyze these different polymorphic forms, DSC was carried out, and to accurately identifying these phases, WAXD is employed, since it allows a better differentiation of each phase. In addition,

Table 3 Thermal properties of lipids mixtures

Sample	Onset temperature/°C	Melting peak/°C	Heat capacity/J/g	$\Delta T = T_{melting} - T_{onset}$
D4M812/90:10	53.7	59.2	130.0	5.5
D4M812/80:20	51.8	56.3	113.0	4.5
D4M812/70:30	52.8	58.2	106.0	5.4
D4M840/90:10	53.1	58.0	124.0	4.9
D4M840/80:20	49.0	55.8	106.0	6.8
D4M840/70:30	47.1	54.1	94.4	7.0
D8M812/90:10	68.2	72.2	147.0	4.0
D8M812/80:20	67.3	71.4	125.0	4.1
D8M812/70:30	64.9	69.4	110.0	4.5
D8M840/90:10	67.3	71.9	141.0	4.6
D8M840/80:20	62.1	68.1	84.5	6.0
D8M840/70:30	60.3	67.2	90.2	6.9

Table 4 Thermal properties of lipids mixtures after and before tempering

Sample	Before			After		
	T_{onset}/°C	$T_{melting}$/°C	ΔT/°C	T_{onset}/°C	$T_{melting}$/°C	ΔT/°C
D4M812/70:30	52.8	58.2	5.4	51.4	58.1	6.7
D4M840/70:30	47.1	54.1	7.0	47.0	56.4	9.4
D8M812/70:30	64.9	69.4	4.5	66.9	72.1	5.2
D8M840/70:30	60.3	67.2	6.9	64.5	70.8	6.3

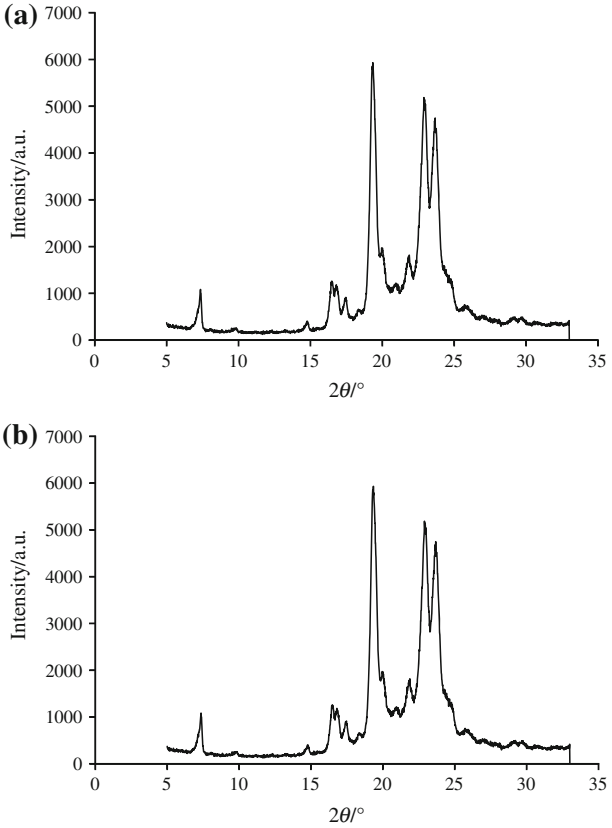

Fig. 1 WAXD analysis after fusion of **a** Dynasan®114 and **b** Dynasan®118

WAXD is used to investigate the arrangement of the layers of lipid molecules and their crystallinity. Figure 1 shows the X-ray diffraction patterns of solid lipids, Dynasan®114 and Dynasan®118. In Fig. 1a the phases α, β, and β'/β are well defined, showing that Dynasan®114 exists in a crystalline state (Fig. 1b). Only one peak at 21.53 (2θ) was recorded, typical of the β-form.

The WAXD diffractogram of Fig. 2 corresponds to the lipid mixtures containing a solid lipid with different ratios of liquid lipid, according to Table 1. In all the cases, there is a clear presence of three crystalline phases (α, β, and β'/β). In the specific case of Dynasan®118, as a bulk material, it shows only one phase (Fig. 1b), but in a mixture with the liquid lipids (Fig. 2a, b), it depicted the three distinct typical phases.

Comparing the baseline (trend linearity) of solid lipid (Fig. 1) with the baselines of the lipid mixtures in Fig. 2, it was also shown that the addition of liquid lipid (Miglyol®812 or Miglyol®840) promoted disorder. From the obtained results, to develop NLC we have chosen the ratio 70:30 (SS:SL), i.e., it is responsible for a greater disorder of the matrix. Therefore, the system shows stability and ability for higher loading. The WAXD diffractogram patterns of Fig. 3 show that after the tempering process of lipid mixtures containing 30% lipid liquid, intensity of the peak is observed. The peak width was maintained, although not as well defined as before the treatment.

Correlating the data obtained by DSC and WAXD after the tempering process, consistent outcomes were observed. The decrease of the melting temperature was followed by the decrease of intensity of WAXD peaks, suggesting the presence of more unorganized structures. This phenomenon is preferred for drug loading and increasing the thermodynamic stability during storage.

PLM analysis compared the morphological characteristics of the lipid mixtures with the samples of solid lipid containing 30% lipid liquid (Fig. 4). The results show the presence of crystalline structures in equilibrium with liquid crystalline lipids. Dynasan®114 and Dynasan®118 are in

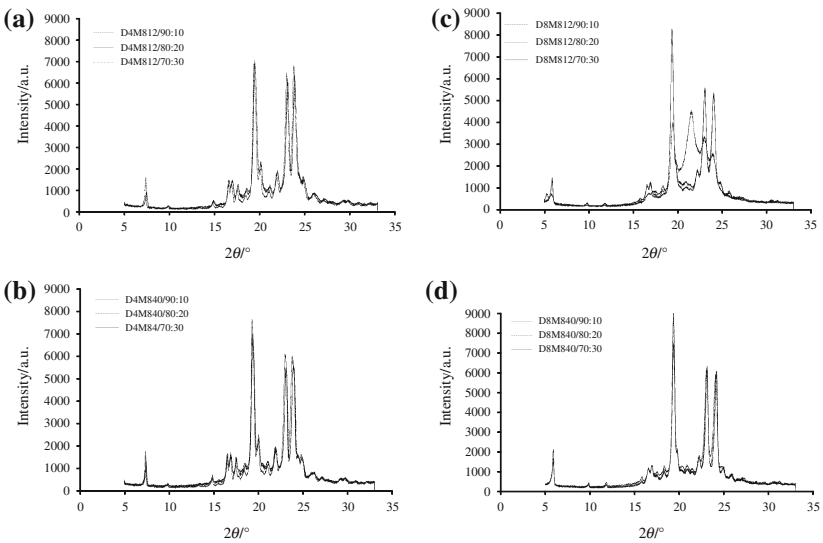

Fig. 2 WAXD analysis after fusion **a** Dynasan®114 and Miglyol®812; **b** Dynasan®114 and Miglyol®840; **c** Dynasan®118 and Miglyol®812; **d** Dynasan®118 and Miglyol®840

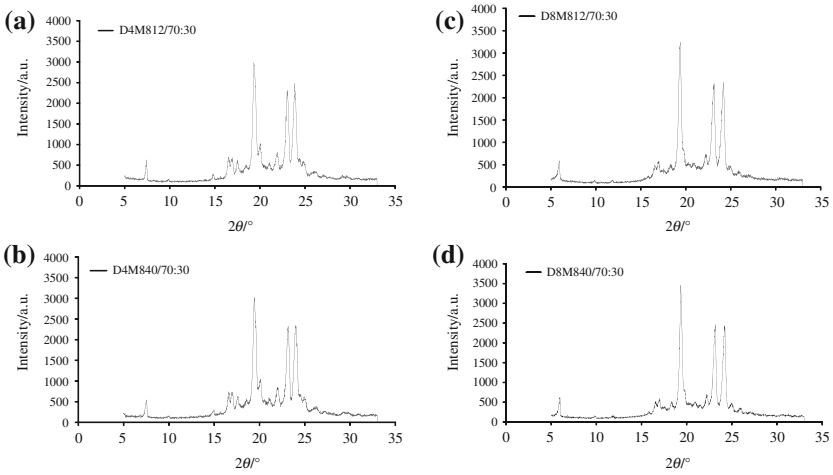

Fig. 3 WAXD analysis after fusion **a** Dynasan®114 and Miglyol®812; **b** Dynasan®114 and Miglyol®840; **c** Dynasan®118 and Miglyol®812; **d** Dynasan®118 and Miglyol®840

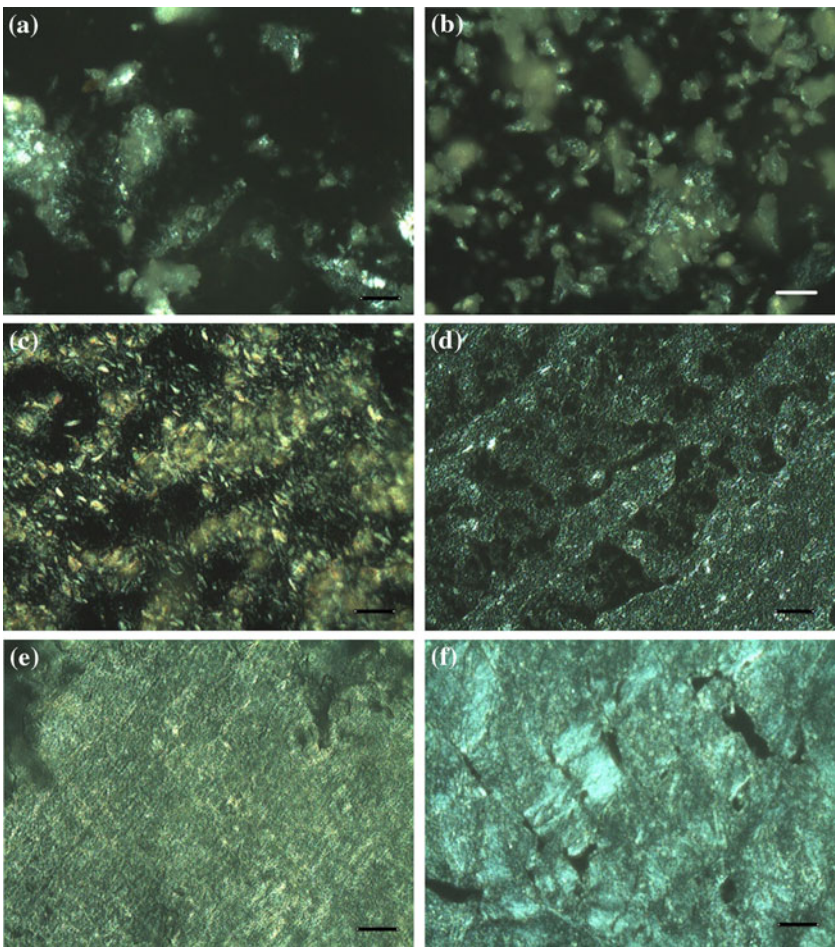

Fig. 4 Micrographs obtained by PLM: **a** Dynasan®114; **b** Dynasan®118; **c** Dynasan®114 and Miglyol®812 (70:30); **d** Dynasan®114 and Miglyol®840 (70:30); **e** Dynasan®118 and Miglyol®812 (70:30); **f** Dynasan®118 e Miglyol®840 (70:30)

the form of irregular crystals of varying sizes. Addition of liquid lipid (30%) created more amorphous structures.

Physicochemical characterization of lipid nanoparticles produced by hot HPH is shown in Table 4. All formulations were obtained with an average hydrodynamic diameter around 200 nm and polydispersity index of 0.329, with the presence of one population. The zeta potential was from −19.26 to +0.25 mV for all formulations with standard deviation in the range of 0.20–0.66. The zeta potential width can be explained by coating the particles with polysorbate 80. This value reveals the particles stability as a result of their interaction with electrolytes and rheology

of colloidal suspensions. While the value was less than |30 mV|, the nanoparticles showed a good level of electrostatic instability, i.e., the electrostatic repulsion prevents aggregation of particles. High surface charges contribute for a long-term stability of nanoparticles both in aqueous dispersion and during their storage and administration [30].

Conclusions

This study was focused on the characterization of lipid mixtures in different concentrations, by DSC, WAXD, and PLM. The results of characterization of the lipid mixtures show that mixtures containing 30% lipid liquid, both for Miglyol®812 and Miglyol®840, were the most promising for the production of the NLC, because of the presence of a more disordered crystal—results that are consistent with the employed technology. The lipid nanoparticles showed size, polydispersity index, and zeta potential promising for drug loading for pharmaceutical and cosmetic use.

Acknowledgements The authors wish to acknowledge the sponsorship of the (FAPESP) Fundação de Amparo e Pesquisa and CAPES (Coordenação de Aperfeiçoamento de Pessoal de Nível Superior). The authors are also thankful to Fundação para a Ciência e Tecnologia do Ministério da Ciência e Tecnologia, under the reference PTDC/SAU-FAR/113100/2009.

References

1. Sahoo SK, Parveen S, Panda JJ. The present and future of nanotechnology in human health care. Nanomedicine. 2007. doi:10.1016/j.nano.2006.11.008.
2. Aji Alex MR, Chacko AJ, Jose S, Souto EB. Lopinavir loaded solid lipid nanoparticles (SLN) for intestinal lymphatic targeting. Eur J Pharm Sci. 2011. doi:10.1016/j.ejps.2010.10.002.
3. Gonzalez-Mira E, Egea MA, Garcia ML, Souto EB. Design and ocular tolerance of flurbiprofen loaded ultrasound-engineered NLC. Colloids Surf B Biointerfaces. 2010. doi:10.1016/j.colsurfb.2010.07.029.
4. Heney M, Alipour M, Vergidis D, Omri A, Mugabe C, Th'ng J, Suntres Z. Effectiveness of liposomal paclitaxel against MCF-7 breast cancer cells. Can J Physiol Pharmacol. 2010. doi:10.1139/y10-097.
5. Wang J, Liu W, Tu Q, Song N, Zhang Y, Nie N. Folate-decorated hybrid polymeric nanoparticles for chemically and physically combined paclitaxel loading and targeted delivery. Biomacromolecules. 2011. doi:10.1021/bm101206g.
6. Barata TS, Shaunak S, Teo I, Zloh M, Brocchini S. Structural studies of biologically active glycosylated polyamidoamine (PAMAM) dendrimers. J Mol Model. 2010. doi:10.1007/s00894-010-0907-1.
7. Rawat MK, Jain A, Singh S. In vivo and cytotoxicity evaluation of repaglinide-loaded binary solid lipid nanoparticles after oral administration to rats. J Pharm Sci. 2011. doi:10.1002/jps.22454.
8. Souto EB, Muller RH. Lipid nanoparticles: effect on bioavailability and pharmacokinetic changes. Handb Exp Pharmacol. 2010. doi:10.1007/978-3-642-00477-3_4.
9. Muller RH, Mader K, Gohla S. Solid lipid nanoparticles (SLN) for controlled drug delivery—a review of the state of the art. Eur J Pharm Biopharm. 2000;50(1):161–77.
10. De Oliveira GG, Ferraz HG, Severino P, Souto EB. Analysis of phase transition and dehydration processes of nevirapine. J Therm Anal Calorim. 2011. doi:10.1007/s10973-011-1424-x.
11. Yoshid MI, Oliveira MA, Gomes ECL, Mussel WN, Castro WV, Soares CDV. Thermal characterization of lovastatin in pharmaceutical formulations. J Therm Anal Calorim. 2011. doi:10.1007/s10973-011-1510-0.
12. Jores K, Mehnert W, Drechsler M, Bunjes H, Johann C, Mader K. Investigations on the structure of solid lipid nanoparticles (SLN) and oil-loaded solid lipid nanoparticles by photon correlation spectroscopy, field-flow fractionation and transmission electron microscopy. J Control Release. 2004. doi:10.1016/j.jconrel.2003.11.012.
13. Bondi ML, Craparo EF, Giammona G, Drago F. Brain-targeted solid lipid nanoparticles containing riluzole: preparation, characterization and biodistribution. Nanomedicine (Lond). 2009. doi:10.2217/nnm.09.67.
14. Souto EB, Muller RH. Investigation of the factors influencing the incorporation of clotrimazole in SLN and NLC prepared by hot high-pressure homogenization. J Microencapsul. 2006. doi:10.1080/02652040500435295.
15. Ali H, Shirode AB, Sylvester PW, Nazzal S. Preparation, characterization, and anticancer effects of simvastatin-tocotrienol lipid nanoparticles. Int J Pharm. 2010. doi:10.1016/j.ijpharm.2010.01.018.
16. Wissing SA, Kayser O, Muller RH. Solid lipid nanoparticles for parenteral drug delivery. Adv Drug Deliv Rev. 2004. doi:10.1016/j.addr.2003.12.002.
17. Muchow M, Maincent P, Muller RH. Lipid nanoparticles with a solid matrix (SLN, NLC, LDC) for oral drug delivery. Drug Dev Ind Pharm. 2008. doi:10.1080/03639040802130061.
18. Mehnert W, Mader K. Solid lipid nanoparticles: production, characterization and applications. Adv Drug Deliv Rev. 2001;47:165–96.
19. Lippacher A, Muller RH, Mader K. Preparation of semisolid drug carriers for topical application based on solid lipid nanoparticles. Int J Pharm. 2001;214:9–12.
20. Muller RH, Radtke M, Wissing SA. Nanostructured lipid matrices for improved microencapsulation of drugs. Int J Pharm. 2002;242:121–8.
21. Muller RH, Radtke M, Wissing SA. Solid lipid nanoparticles (SLN) and nanostructured lipid carriers (NLC) in cosmetic and dermatological preparations. Adv Drug Deliv Rev. 2002;54:S131–55.
22. Souto EB, Mehnert W, Muller RH. Polymorphic behaviour of Compritol888 ATO as bulk lipid and as SLN and NLC. J Microencapsul. 2006. doi:10.1080/02652040600612439.
23. Potta SG, Minemi S, Nukala RK, Peinado C, Lamprou DA, Urquhart A, Douroumis D. Preparation and characterization of ibuprofen solid lipid nanoparticles with enhanced solubility. J Microencapsul. 2011. doi:10.3109/02652048.2010.529948.
24. Luykx DM, Peters RJ, van Ruth SM, Bouwmeester H. A review of analytical methods for the identification and characterization of nano delivery systems in food. J Agric Food Chem. 2008. doi:10.1021/jf8013926.
25. Rica RA, Jiménez ML, Delgado AV. Dynamic mobility of rod-like goethite particles. Langmuir. 2009. doi:10.1021/la9013976.
26. Jenning V, Thunemann AF, Gohla SH. Characterisation of a novel solid lipid nanoparticle carrier system based on binary mixtures of liquid and solid lipids. Int J Pharm. 2000;199:167–77.
27. Mezzena M, Scalia S, Young PM, Traini D. Solid lipid budesonide microparticles for controlled release inhalation therapy. AAPS J. 2009. doi:10.1208/s12248-009-9148-6.

28. Kim JK, Park JS, Kim CK. Development of a binary lipid nanoparticles formulation of itraconazole for parenteral administration and controlled release. Int J Pharm. 2010. doi:10.1016/j.ijpharm.2009.09.008.
29. Attama AA, Muller-Goymann CC. Investigation of surface-modified solid lipid nanocontainers formulated with a heterolipid-templated homolipid. Int J Pharm. 2007. doi:10.1016/j.ijpharm.2006.10.032.
30. Bayindir ZS, Yuksel N. Characterization of niosomes prepared with various nonionic surfactants for paclitaxel oral delivery. J Pharm Sci. 2010. doi:10.1002/jps.21944.